Atmospheric
Measurement
Techniques

Supplement of

Response of protonated, adduct, and fragmented ions in Vocus proton-transfer-reaction time-of-flight mass spectrometer (PTR-ToF-MS)

Fangbing Li et al.

Correspondence to: Yong Jie Li (yongjieli@um.edu.mo)

List of the supporting information:

Tables.

Figures.

110   **Tables.**

111   **Table S1.** The details of instrument setting experiments.

Varying setting	Vocus front (volt)	Vocus back (volt)	pressure (mbar)	E/N (Td)	BSQ (volt)	RF (volt)
E	300 to 700	34	2	48 to 142	260	500
N	500	34	1.5 to 3.5	57 to 133	260	500
RF	700	34	2	171	260	500 to 13
BSQ	700	34	2	171	300 to 50	500
RF	700	34	3.5	98	260	500 to 13
BSQ	700	34	3.5	98	300 to 50	500

112

113 **Table S2.** Details of the tested volatile organic compounds (VOCs). Also shown are their
114 proton affinity (PA) values.

Group[a]	Name	CAS#	m/Q (Th)[b] Exact	m/Q (Th)[b] Measured	PA (kJ mol^{-1})[c]
A1	Benzene	71-43-2	79.0542	79.0548	750.4
	Toluene	108-88-3	93.0699	93.0699	784
	m-Xylene	108-38-3	107.0855	107.0859	812.1
	1,2,4-Trimethylbenzene	95-63-6	121.1012	121.1007	798.3
A2	Isoprene	78-79-5	69.0699	69.0709	826.4
	α-Pinene	80-56-8	137.1325	137.1321	878.6[d]
	β-Caryophyllene	87-44-5	205.1951	205.198	859.2[e]
B1	Formaldehyde	50-00-0	31.0178	31.0171	712.5
	Acetaldehyde	75-07-0	45.0335	45.0329	768.5
B2	n-Butanal	123-72-8	73.0648	73.0656	792.7
	Pentanal	110-62-3	87.0804	87.0802	796.6
	Hexaldehyde	66-25-1	101.0961	101.0957	794.4~797[f]
B3	Acetone	67-64-1	59.0491	59.0491	812
	Methyl ethyl Ketone	78-93-3	73.0648	73.0656	827.3
B4	Acrolein	107-02-8	57.0335	57.0332	797
	Methacrolein	78-85-3	71.0491	71.0495	808.7
B5	Benzaldehyde	100-52-1	107.0491	107.0504	834
	m-Tolualdehyde	620-23-5	121.0648	121.0651	840
C1	Acetonitrile	75-05-8	42.0338	42.0329	779.2
	Acrylonitrile	107-13-1	54.0338	54.0334	784.7
C2	Methanol	67-56-1	33.0335	33.0323	754.3

115 Notes:
116 a, A1: aromatic hydrocarbons, A2: terpenoids, B1: small aldehydes; B2: long-chain aldehydes, B3: ketones, B4:
117 unsaturated aldehydes, B5: aromatic aldehydes, C1: nitriles, C2: methanol;
118 b, mass-to-charge ratio of protonated ion MH$^+$;
119 c, taken from NIST Chemistry WebBook William E. Acree and Chickos (2023), unless stated otherwise;
120 d, from Solouki and Szulejko (2007); e, from Jenkin et al. (2012); f, from Blake et al. (2008).
121

Table S3. Proton-transfer reaction rate constants (k_{ptr}, × 10⁻⁹ cm³ molec⁻¹ s⁻¹) from literature.

Group	Name	k_{model}^a	$k_{experiment}^b$					N^c	k_{avg}^d	k_{std}^e
A1	Benzene	1.97	1.8	1.9	2.1	1.85	—	5	1.92	0.13
	Toluene	2.12	2.05	1.9	2.2	2.3	—	5	2.11	0.14
	m-Xylene	2.26	2.3	—	—	—	—	2	2.28	0.24
	1,2,4-Trimethylbenzene	2.4	2.4	—	—	—	—	2	2.4	0.25
A2	Isoprene	1.94	1.3	2	2	1.7	2.1	6	1.84	0.12
	α-Pinene	2.44	2.2	2.6	—	—	—	3	2.41	0.22
	β-Caryophyllene	3.1	—	—	—	—	—	1	3.1	0.47
B1	Formaldehyde	3	3.4	—	—	—	—	2	3.2	0.35
	Acetaldehyde	3.36	3.5	3.6	3.7	—	—	4	3.54	0.27
B2	n-Butanal	3.49	3.8	—	—	—	—	2	3.65	0.39
	Pentanal	3.34	3.6	—	—	—	—	2	3.47	0.37
	Hexaldehyde	3.74	3.7	—	—	—	—	2	3.72	0.39
B3	Acetone	3	2.4	3.59	3.9	4.1	—	5	3.4	0.26
	Methyl ethyl Ketone	3.83	3.03	3.9	—	—	—	3	3.59	0.34
B4	Acrolein	3.35	4.2	—	—	—	—	2	3.78	0.45
	Methacrolein	3.55	—	—	—	—	—	1	3.55	0.53
B5	Benzaldehyde	4.12	3.7	—	—	—	—	2	3.91	0.43
	m-Tolualdehyde	4.9	4.1	—	—	—	—	2	4.5	0.52
C1	Acetonitrile	4.74	2.7	4.7	5.1	3.92	—	5	4.23	0.33
	Acrylonitrile	5.1	—	—	—	—	—	1	5.1	0.77
C2	Methanol	2.33	2.1	2.2	2.7	—	—	4	2.33	0.18

Notes:
a, From Zhao and Zhang (2004);
b, From Pagonis et al. (2019) and reference therein, as well as Zhao and Zhang (2004), , Michel et al. (2005), Milligan et al. (2002), Lindinger et al. (1998), Cappellin et al. (2012), Sekimoto et al. (2017);
c, number of values for averaging;
d, averaged $k_{proton-transfer}$;
e, the uncertainty of $k_{proton-transfer}$ by assuming 15% uncertainty for modeled values Zhao and Zhang (2004) as well as experiment values, weighted by the number of values.

Table S4. The RH dependence, sensitivity, intercept of protonated adducts, and fragmented ions.

Group	Name	[MH+H₂O]⁺ Sensitivity (cps/ppbv)	Intercept (cps)	RH-dependence (%)	[MH-H₂O]⁺ Sensitivity (cps/ppbv)	Intercept (cps)	RH-dependence (%)	[MH-CₓHᵧ]⁺ Sensitivity (cps/ppbv)	Intercept (cps)	RH-dependence (%)	Signal percentage (%)[b] MH⁺	[MH+H₂O]⁺	[MH-H₂O]⁺	[MH-CₓHᵧ]⁺
A1	Benzene	—[a]	—	—	—	—	—	—	—	—	100	—	—	—
	Toluene	—	—	—	—	—	—	153.7	52.7	-1.5	98	—	—	2
	m-Xylene	—	—	—	—	—	—	2903.7	-168.1	-0.8	76	—	—	24
	1,2,4-Trimethylbenzene	—	—	—	—	—	—	1219.8	-185.5	-0.4	88	—	—	12
A2	Isoprene	—	—	—	—	—	—	154.4	211.9	-1.1	93	—	—	7
	α-Pinene	—	—	—	—	—	—	4171.2	1437.7	0.2	46	—	—	54
	β-Caryophyllene	1.4	1.7	3.5	—	—	—	—	—	—	100	—	—	<<1[d]
B1	Formaldehyde	—	—	—	—	—	—	—	—	—	100	—	—	—
	Acetaldehyde I[c]	—	—	—	0.1	0.6	-0.79	—	—	—	100	—	<<1[d]	—
	Acetaldehyde II[c]	—	—	—	0.2	0.6	0.67	—	—	—	100	—	<<1[d]	—
B2	n-Butanal	201.4	327.5	5.1	5589.1	13531	0.02	—	—	—	23	3	75	?[e]
	Pentanal	1300.1	1617.1	1.4	4116.6	816.3	0.29	—	—	—	24	7	69	?
	Hexaldehyde	367	399.3	8.2	367	399.3	0.30	84	1203.6	0.6	20	6	72	2
B3	Acetone I[c]	58	433	5.4	288.1	635	0.37	131	5939.7	-3.0	91	1	3	5
	Acetone II[c]	64.5	444.3	5.3	603.5	556.6	0.38	170.9	5674.8	-2.1	91	1	3	5
	Methyl ethyl Ketone	273.4	178.3	2.8	1084.3	13728.2	-0.92	208.2	2614.9	0.2	77	2	17	2
B4	Acrolein	49.7	4057	2.3	268.7	339.2	0.47	—	—	—	91	5	4	—
	Methacrolein	385.5	746.5	2.3	217.5	176.6	-0.19	—	—	—	90	7	3	—
B5	Benzaldehyde	774.9	-457.7	2.7	—	—	—	—	—	—	95	5	—	—
	m-Tolualdehyde	985	-956.1	2.4	—	—	—	1261	742.5	-2.4	87	8	—	6
C1	Acetonitrile	46.2	1199.8	8.5	—	—	—	—	—	—	93	7	—	—
	Acrylonitrile	118.2	111	5.2	—	—	—	—	—	—	99	1	—	—
C2	Methanol	40.7	0.69	1.9	—	—	—	—	—	—	3	97	—	—

Notes:
a, not available;
b, the specific percentage of fragment or adducted ion signals on all ion signals;
c, from gas standard cylinders I and II.
d, far less than 1 and closer to zero;
e, not determined due to overlapping signals.

139 **Figures.**

140
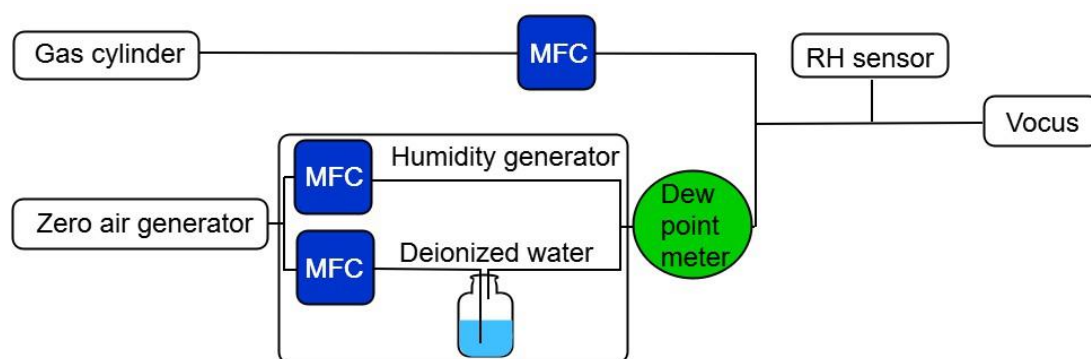
141 **Figure S1.** The diagram of the RH experimental setup. MFC: mass flow controller.
142
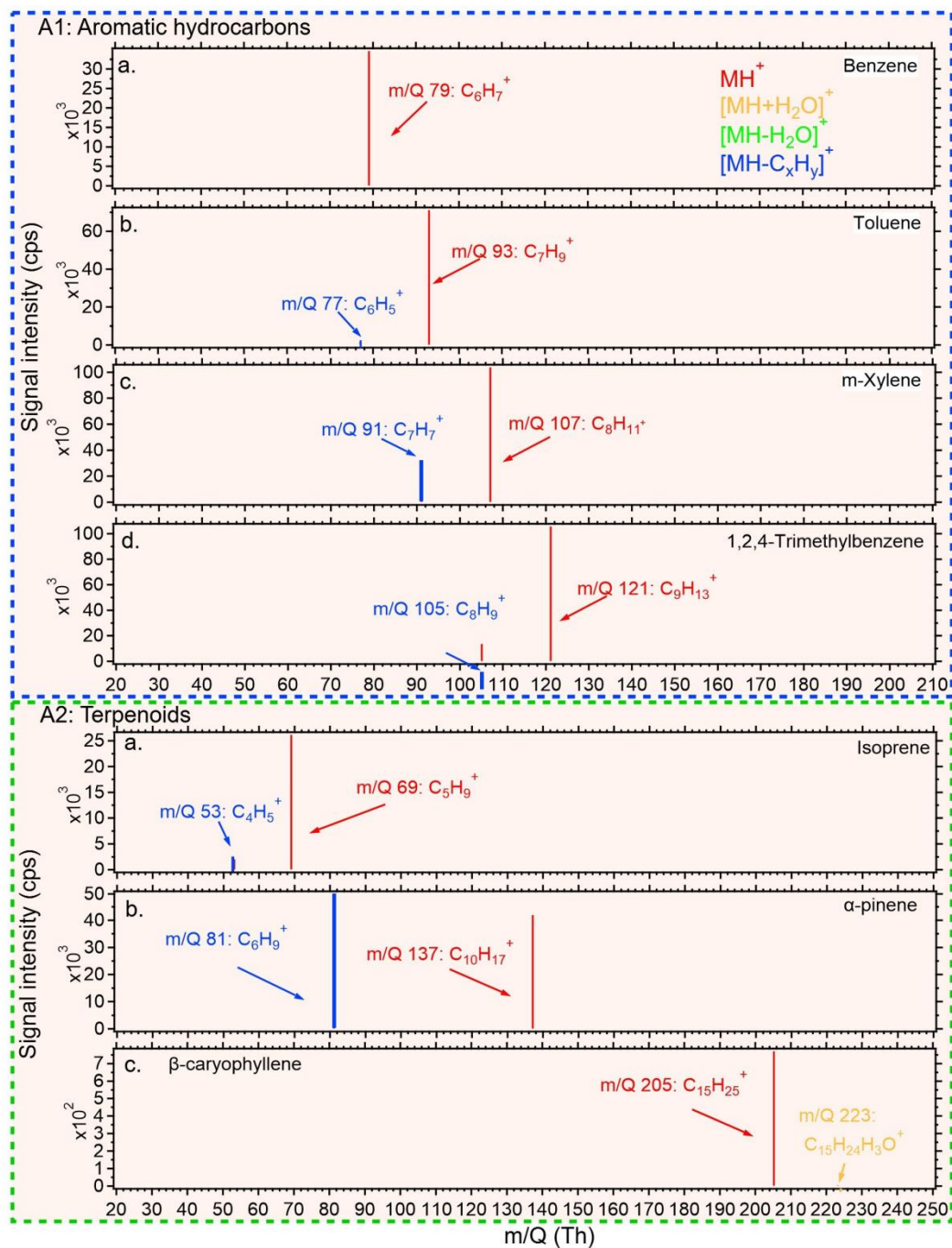
Figure S2. The mass spectra of aromatic hydrocarbons (benzene, toluene, m-xylene, and 1,2,4-trimethylbenene), and terpenoids (isoprene, α-pinene, and β-caryophyllene) in Vocus at a mixing ratio of ~ 12 ppbv (β-caryophyllene 1.2 ppbv).
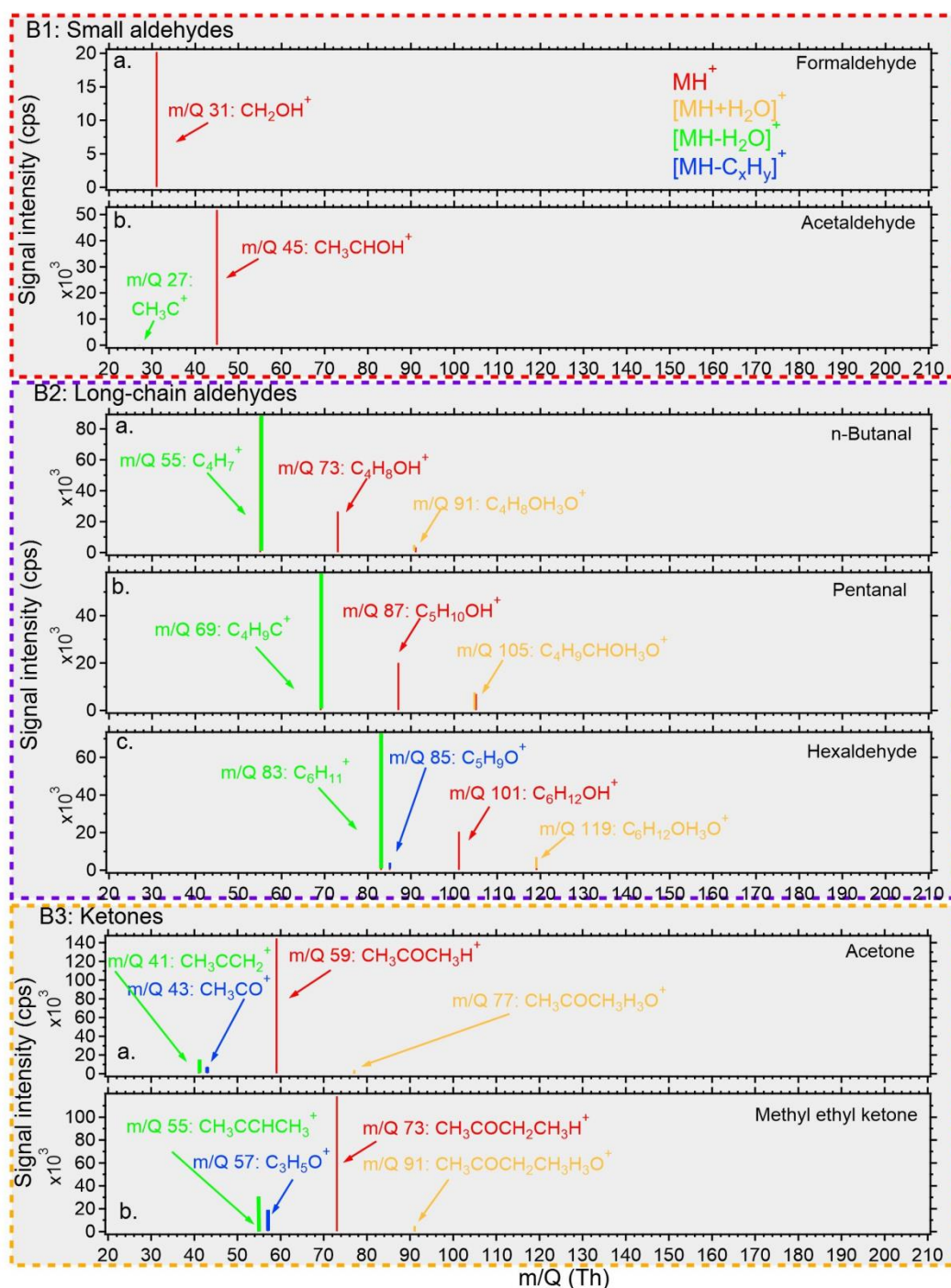
Figure S3. The mass spectra of small aldehydes (formaldehyde and acetaldehyde), long-chain aldehydes (n-butanal, pentanal, and hexaldehyde), and ketones (acetone, and methyl ethyl ketone) in Vocus at a mixing ratio of ~ 12 ppbv.
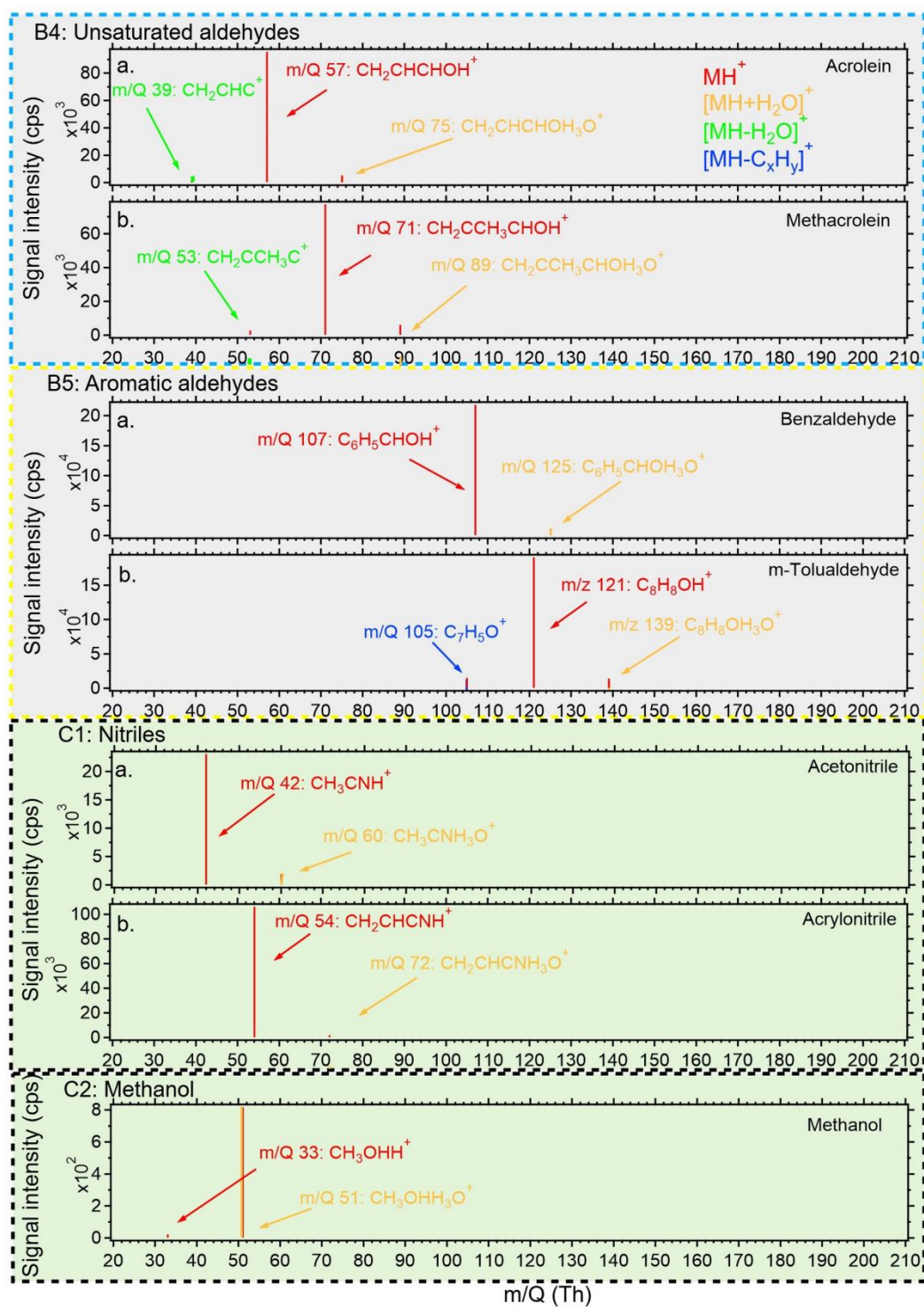
Figure S4. The mass spectra of unsaturated aldehydes (acrolein and methacrolein), aromatic aldehydes (benzaldehyde and m-tolualdehyde), nitriles (acetonitrile and acrylonitrile), and methanol in Vocus at a mixing ratio of ~ 12 ppbv.
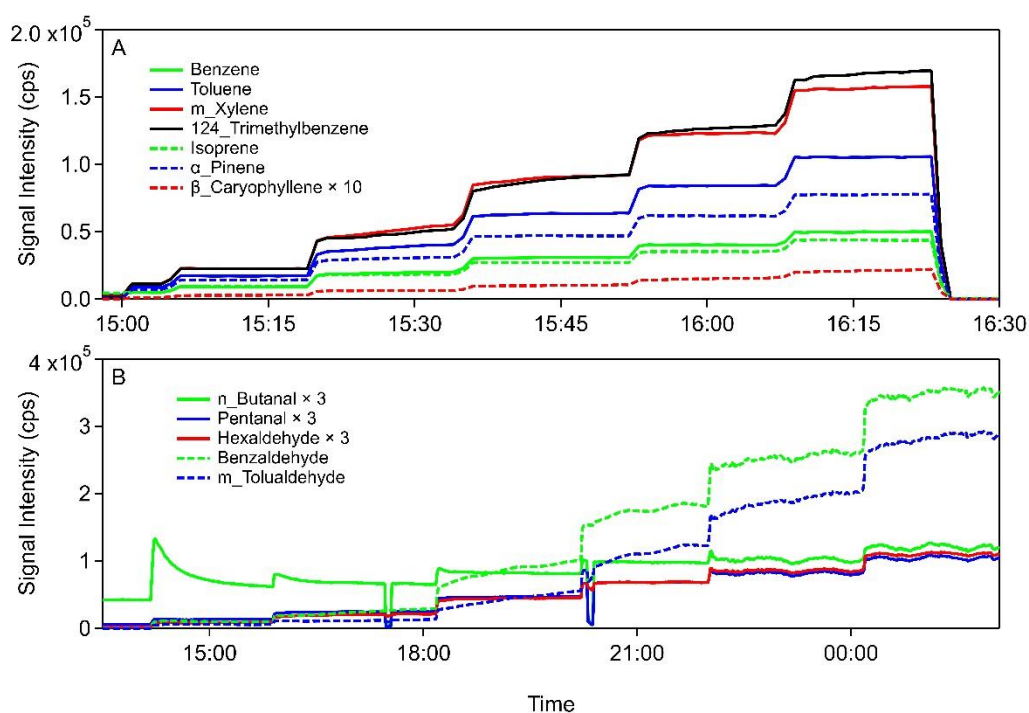
Figure S5. Time series of the protonated ion (MH⁺) signals for selected (A) VOCs and (B) OVOCs as concentration varied from 0 to ~22 ppbv (~2 ppbv for β caryophyllene) under dry (MH ~5%) conditions. Note the signals were magnified by 10 times for β-caryophyllene and 3 times for n-butanal, pentanal, and hexaldehyde.
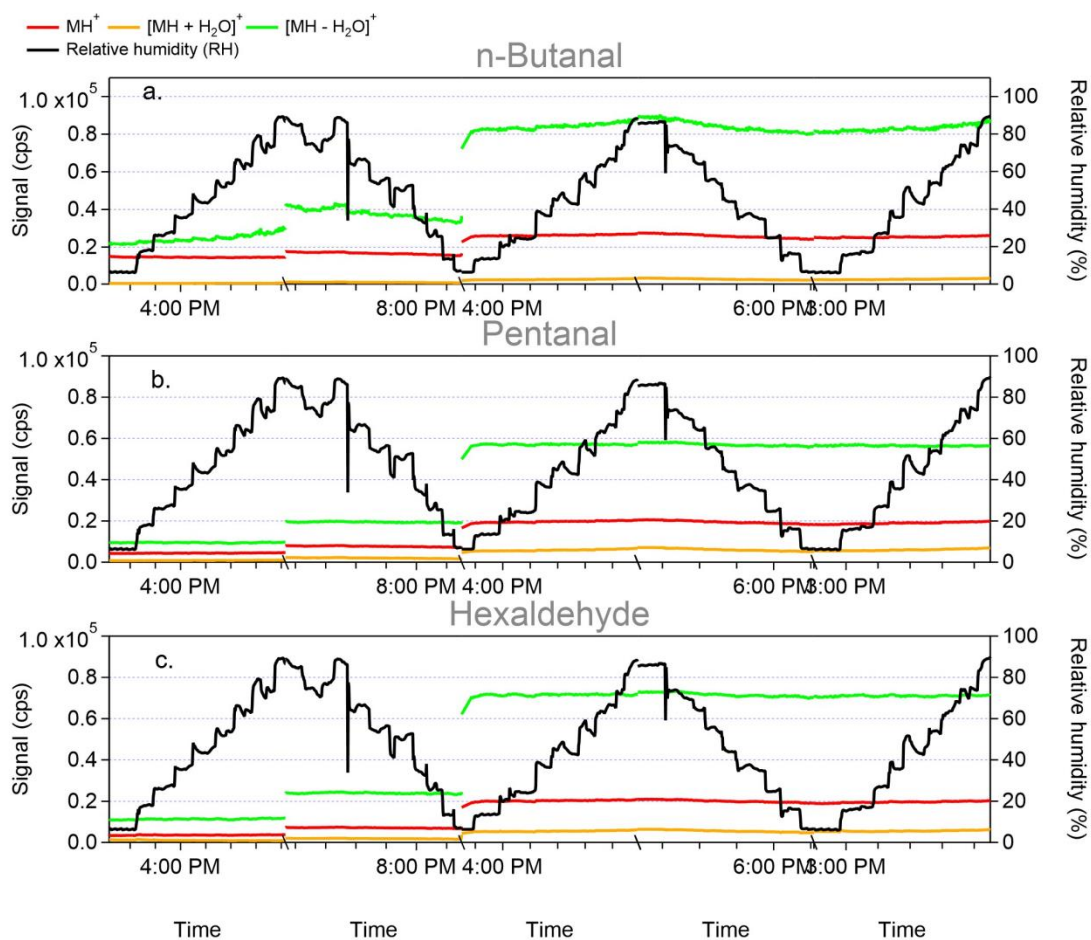
Figure S6. Time series of the protonated ion (MH⁺), adduct ions ([MH + H₂O]⁺), and fragmented ions ([MH − H₂O]⁺) and/or ([MH − CₓHᵧ]⁺) signals for n-butanal, pentanal, and hexaldehyde. Note that the time in x axis is not continuous, with some periods with noisy signals cut off.

Figure S7. The signal intensities (panels a, b, and c, and panels g, h, and i) and fractions (panels d, e, and f, and panels j, k, and l) of protonated ion (MH$^+$), adduct ions ([MH + H$_2$O]$^+$), and fragmented ions ([MH − H$_2$O]$^+$ and [MH − C$_x$H$_y$]$^+$) for α-pinene as functions of E/N ratio (a, d, g, and j), RF amplitude (b, e, h, and k), and BSQ amplitude (c, f, i, and l). The difference between a/d and g/j is that the former fixed N (p = 2.0 mbar) and varied axial voltage (V) to change E/N ratio, while the latter fixed V (= 466 volts) and varied p (i.e., N) to change E/N ratio. The difference between b/e and h/k and between c/f and i/l is that the former was at p = 2.0 mbar while the latter p = 3.5 mbar. If not varied, RF amplitude was set at 500 volts and BSQ amplitude at 300 volts.

Figure S8. The signal intensities (panels a, b, and c, and panels g, h, and i) and fractions (panels d, e, and f, and panels j, k, and l) of protonated ion (MH$^+$), adduct ions ([MH + H$_2$O]$^+$), and fragmented ions ([MH – H$_2$O]$^+$ and [MH – C$_x$H$_y$]$^+$) for 1,2,4-trimethylbenzene as functions of E/N ratio (a, d, g, and j), RF amplitude (b, e, h, and k), and BSQ amplitude (c, f, i, and l). The difference between a/d and g/j is that the former fixed N (p = 2.0 mbar) and varied axial voltage (V) to change E/N ratio, while the latter fixed V (= 466 volts) and varied p (i.e., N) to change E/N ratio. The difference between b/e and h/k and between c/f and i/l is that the former was at p = 2.0 mbar while the latter p = 3.5 mbar. If not varied, RF amplitude was set at 500 volts and BSQ amplitude at 300 volts.
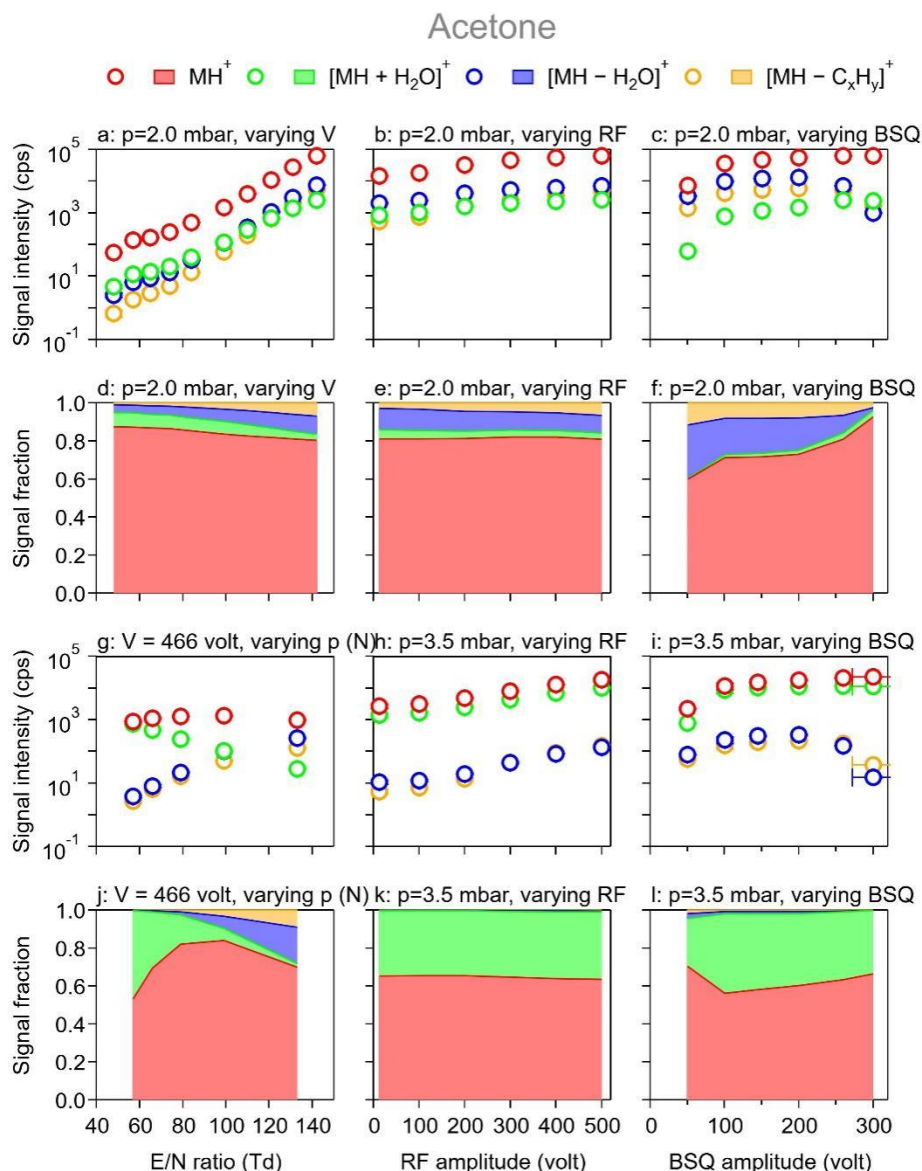
Figure S9. The signal intensities (panels a, b, and c, and panels g, h, and i) and fractions (panels d, e, and f, and panels j, k, and l) of protonated ion (MH^+), adduct ions ($[MH + H_2O]^+$), and fragmented ions ($[MH - H_2O]^+$ and $[MH - C_xH_y]^+$) for acetone as functions of E/N ratio (a, d, g, and j), RF amplitude (b, e, h, and k), and BSQ amplitude (c, f, i, and l). The difference between a/d and g/j is that the former fixed N (p = 2.0 mbar) and varied axial voltage (V) to change E/N ratio, while the latter fixed V (= 466 volts) and varied p (i.e., N) to change E/N ratio. The difference between b/e and h/k and between c/f and i/l is that the former was at p = 2.0 mbar while the latter p = 3.5 mbar. If not varied, RF amplitude was set at 500 volts and BSQ amplitude at 300 volts.

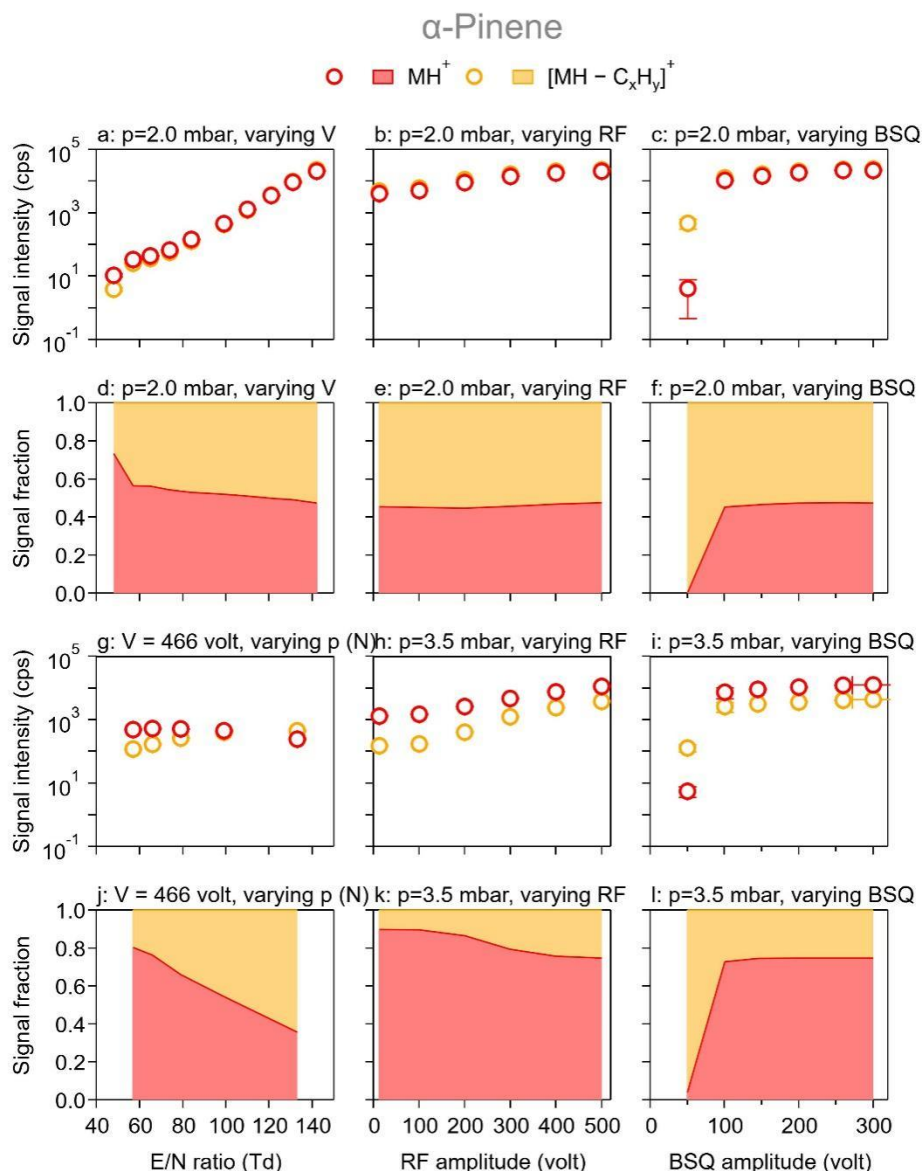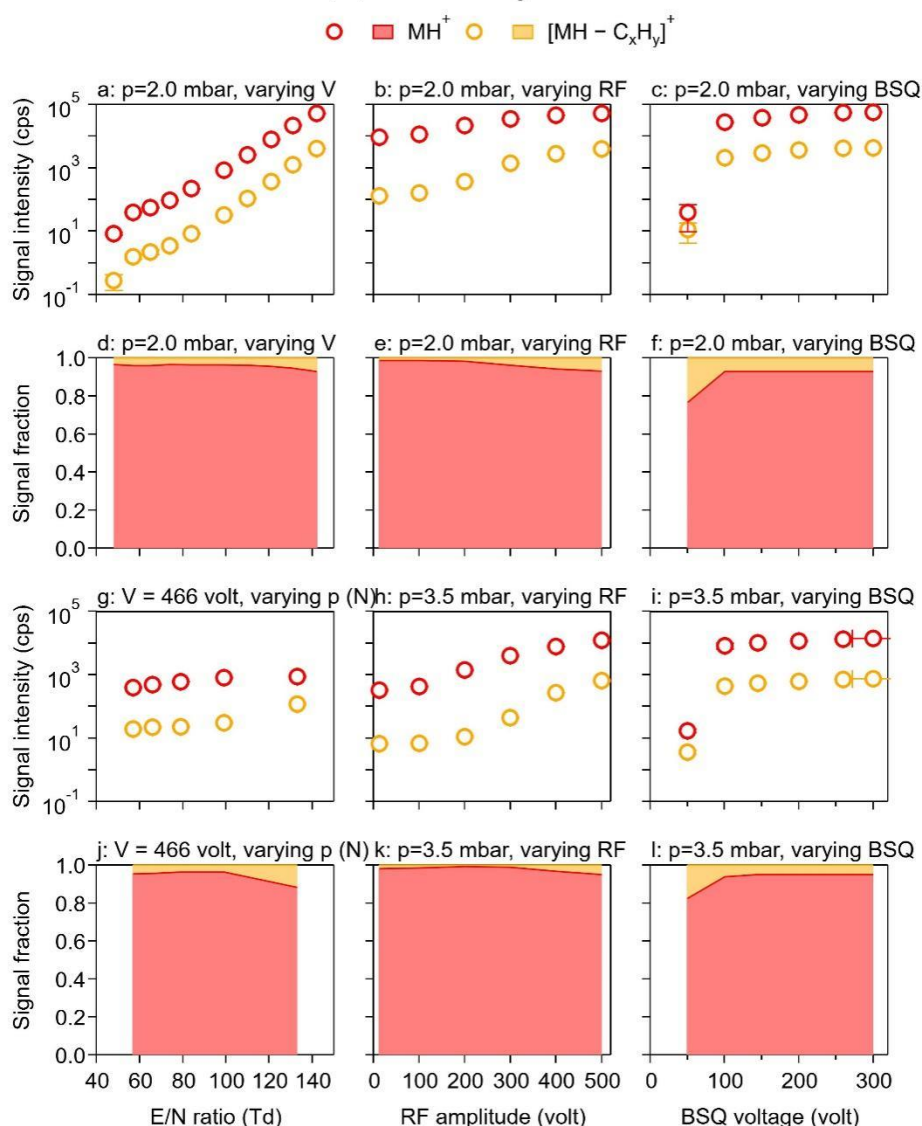**Figure S10.** The signal intensities (panels a, b, and c, and panels g, h, and i) and fractions (panels d, e, and f, and panels j, k, and l) of protonated ion (MH$^+$), adduct ions ([MH + H$_2$O]$^+$), and fragmented ions ([MH − H$_2$O]$^+$ and [MH − C$_x$H$_y$]$^+$) for hexaldehyde as functions of E/N ratio (a, d, g, and j), RF amplitude (b, e, h, and k), and BSQ amplitude (c, f, i, and l). The difference between a/d and g/j is that the former fixed N (p = 2.0 mbar) and varied axial voltage (V) to change E/N ratio, while the latter fixed V (= 466 volts) and varied p (i.e., N) to change E/N ratio. The difference between b/e and h/k and between c/f and i/l is that the former was at p = 2.0 mbar while the latter p = 3.5 mbar. If not varied, RF amplitude was set at 500 volts and BSQ amplitude at 300 volts.
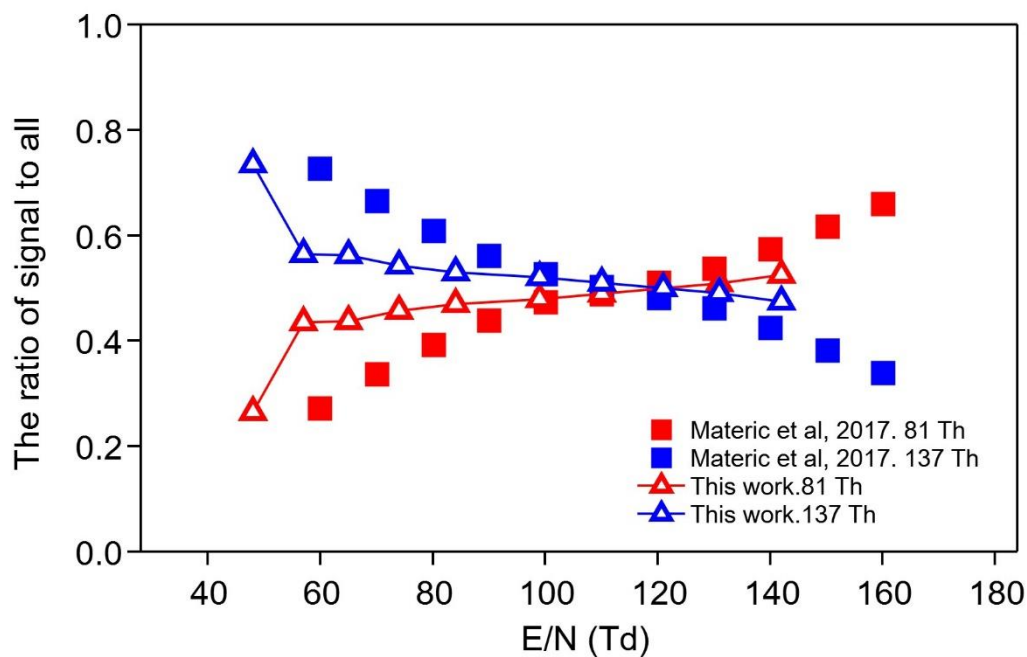
216
217 **Figure S11.** The ratio of α-pinene signals (MH$^+$: 137 Th; [MH – C$_x$H$_y$]$^+$: 81 Th) to all

218 ion signals. This was used to estimate the E/N ratio.
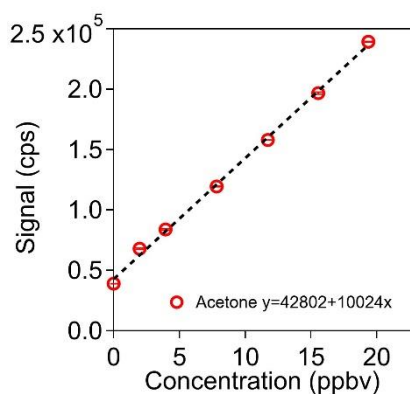
219
220 **Figure S12.** The sensitivity of acetone. An intercept above zero indicates a high

221 background value.
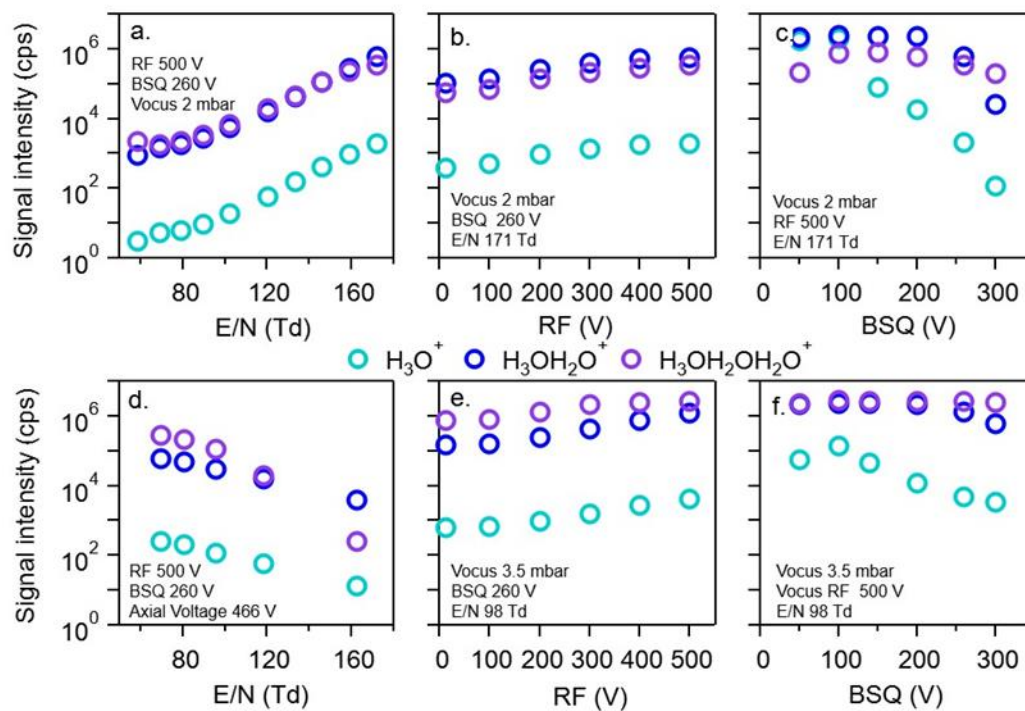
Figure S13. The signal intensities of H_3O^+, $H_3OH_2O^+$, and $H_3O(H_2O)_2^+$ as conditions varied as in Figures 3 in the main text and S14 below.
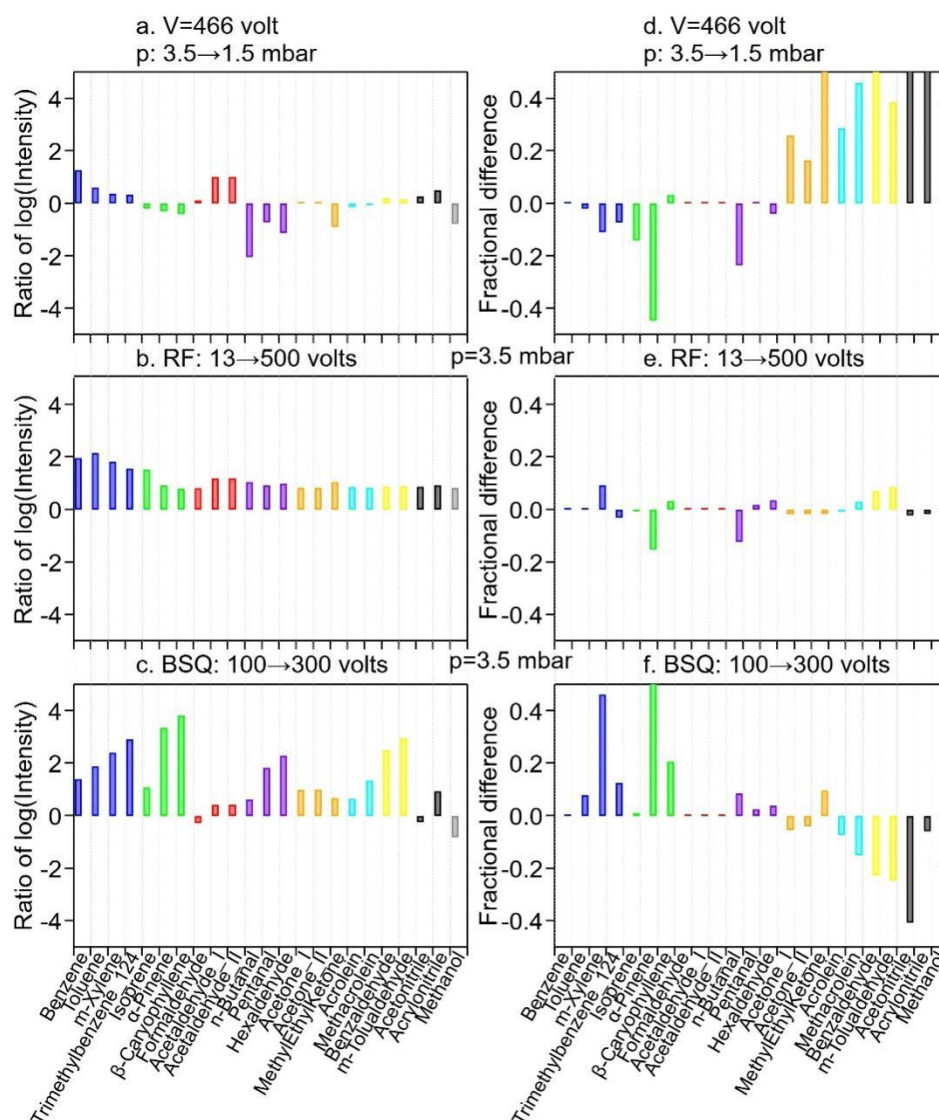
226
227 **Figure S14.** The ratio of the logarithm of intensity (panels a, b, and c) and the difference
228 of fractional signal of the protonated ion (MH$^+$) among all ions (panels d, e, and f),
229 when changing axial voltage (V) or FIMR pressure (p) (panels a and d), RF amplitude
230 (panels b and e), and BSQ amplitude (panels c and f). The ratios were taken after taking
231 the logarithm of the signal intensities of MH$^+$ at the right-hand side of the instrument
232 setting (after the arrow) to that at the left-hand side of the instrument setting stated in
233 the panel label; likewise, the fractional differences are the fractions of the MH$^+$ signal
234 among the protonated, fragmented, and adduct signals under these two instrumental
235 settings.

236
237
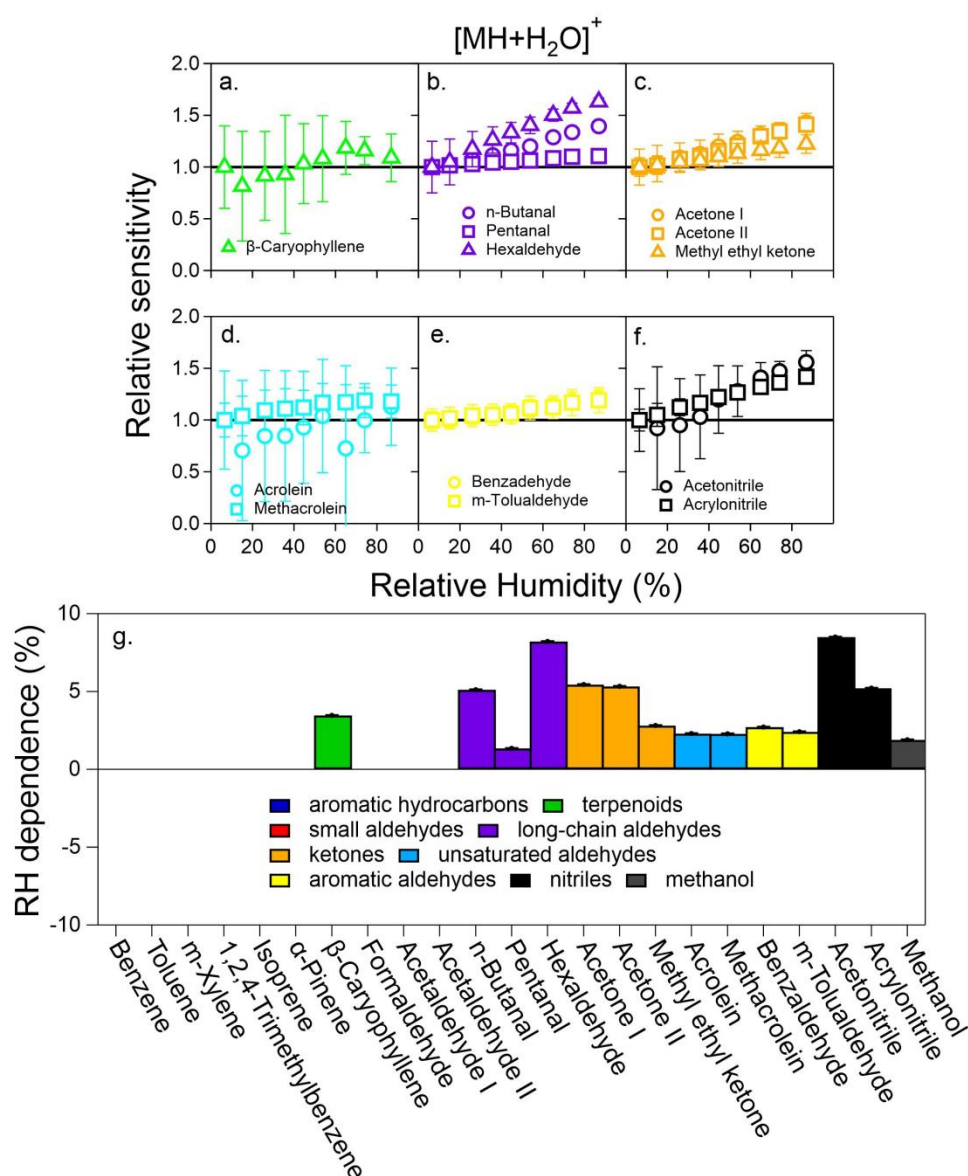
Figure S15. The dependence of the $[MH+H_2O]^+$ signals on RH for the VOCs studied. Panels a-f: the relative sensitivity was calculated as the slope (sensitivity) under high-RH conditions to that at the dry (RH<5%) condition. Panel g: the percent change of relative sensitivity per 10% RH increase.
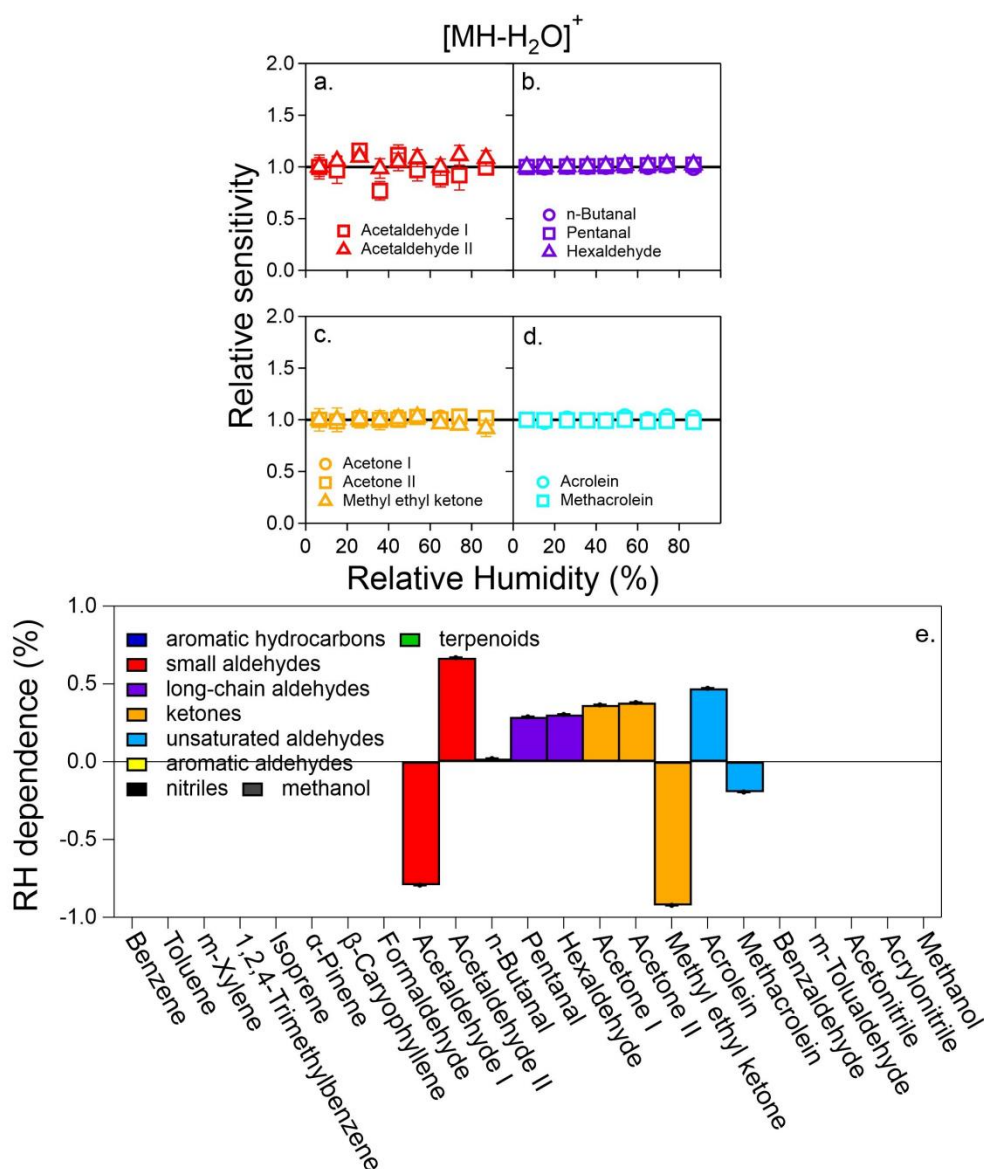
Figure S16. The dependence of the $[MH-H_2O]^+$ signals on RH for the VOCs and OVOCs. Panels a-d: the relative sensitivity was calculated as the slope (sensitivity) under high-RH conditions to that at the dry (RH<5%) condition. Panel e: the percent change of relative sensitivity per 10% RH increase.

Figure S17. The dependence of the $[MH-C_xH_y]^+$ signals on RH for the VOCs and OVOCs tested at a concentration of ~12 ppbv. Panels a-e: the relative sensitivity was calculated as the slope (sensitivity) under high-RH conditions to that at the dry (RH<5%) condition. Panel f: the percent change of relative sensitivity per 10% RH increase.
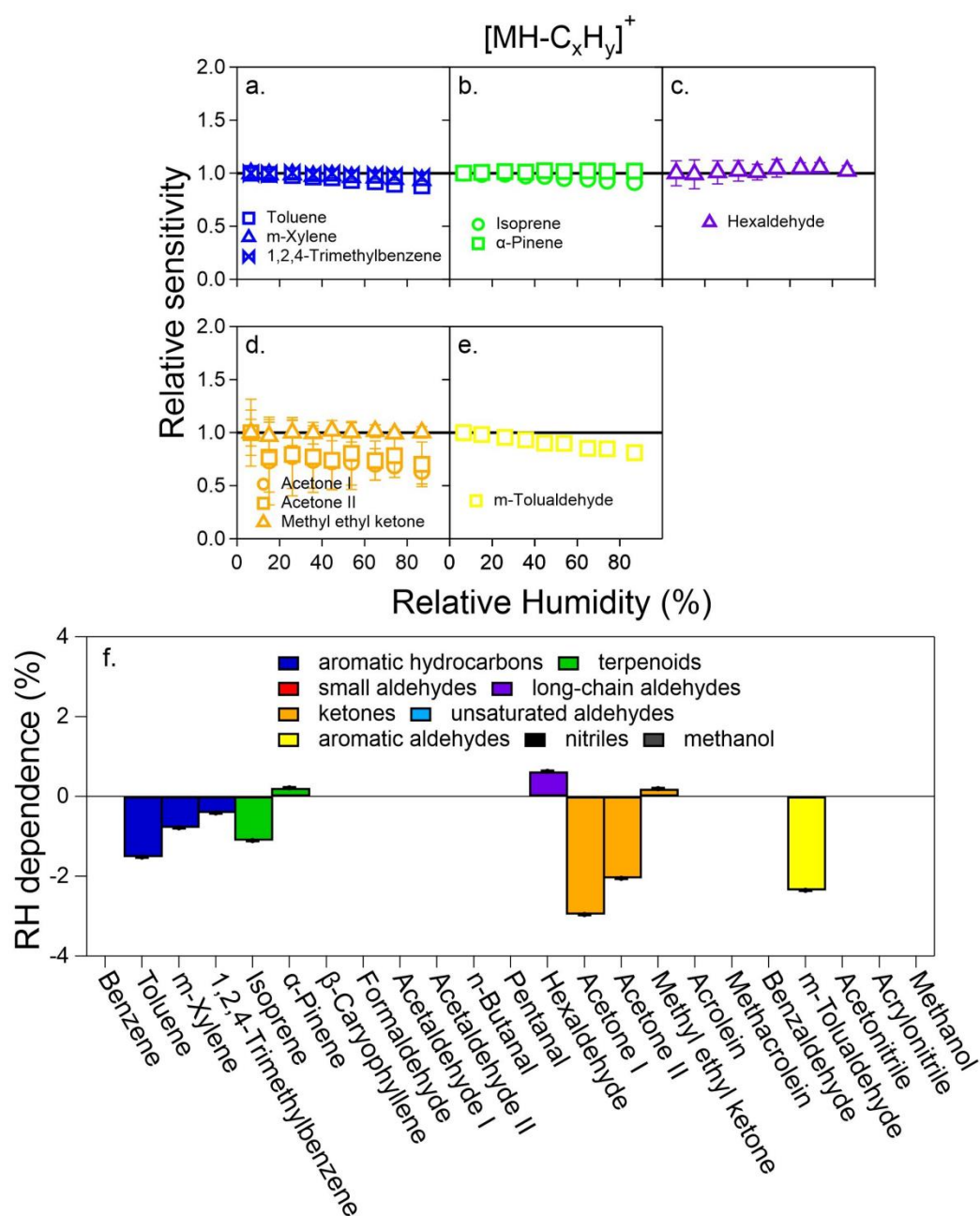
References

Blake, R. S., Patel, M., Monks, P. S., Ellis, A. M., Inomata, S., and Tanimoto, H.: Aldehyde and ketone discrimination and quantification using two-stage proton transfer reaction mass spectrometry, International Journal of Mass Spectrometry, 278, 15-19, https://doi.org/10.1016/j.ijms.2008.07.010, 2008.

Cappellin, L., Karl, T., Probst, M., Ismailova, O., Winkler, P. M., Soukoulis, C., Aprea, E., Märk, T. D., Gasperi, F., and Biasioli, F.: On Quantitative Determination of Volatile Organic Compound Concentrations Using Proton Transfer Reaction Time-of-Flight Mass Spectrometry, Environmental Science & Technology, 46, 2283-2290, https://doi.org/10.1021/es203985t, 2012.

Jenkin, M. E., Wyche, K. P., Evans, C. J., Carr, T., Monks, P. S., Alfarra, M. R., Barley, M. H., McFiggans, G. B., Young, J. C., and Rickard, A. R.: Development and chamber evaluation of the MCM v3.2 degradation scheme for β-caryophyllene, Atmos. Chem. Phys., 12, 5275-5308, https://doi.org/10.5194/acp-12-5275-2012, 2012.

Lindinger, W., Hansel, A., and Jordan, A.: On-line monitoring of volatile organic compounds at pptv levels by means of proton-transfer-reaction mass spectrometry (PTR-MS) medical applications, food control and environmental research, Int J Mass Spectrom, 173, 191-241, https://doi.org/10.1016/S0168-1176(97)00281-4, 1998.

Michel, E., Schoon, N., Amelynck, C., Guimbaud, C., Catoire, V., and Arijs, E.: A selected ion flow tube study of the reactions of H3O+, NO+ and O2+ with methyl vinyl ketone and some atmospherically important aldehydes, International Journal of Mass Spectrometry, 244, 50-59, https://doi.org/10.1016/j.ijms.2005.04.005, 2005.

Milligan, D. B., Wilson, P. F., Freeman, C. G., Meot-Ner, M., and McEwan, M. J.: Dissociative proton transfer reactions of H3+, N2H+, and H3O+ with acyclic, cyclic, and aromatic hydrocarbons and nitrogen compounds, and astrochemical implications, The Journal of Physical Chemistry A, 106, 9745-9755, https://org.doi/10.1021/jp014659i, 2002.

Pagonis, D., Sekimoto, K., and de Gouw, J.: A Library of Proton-Transfer Reactions of H3O+ Ions Used for Trace Gas Detection, J Am Soc Mass Spectr, 30, 1330-1335, 2019.

Sekimoto, K., Li, S. M., Yuan, B., Koss, A., Coggon, M., Warneke, C., and de Gouw, J.: Calculation of the sensitivity of proton-transfer-reaction mass spectrometry (PTR-MS) for organic trace gases using molecular properties, International Journal of Mass Spectrometry, 421, 71-94, 2017.

Solouki, T. and Szulejko, J. E.: Bimolecular and unimolecular contributions to the disparate self-chemical ionizations of α-Pinene and camphene isomers, J Am Soc Mass Spectr, 18, 2026-2039, https://doi.org/10.1016/j.jasms.2007.08.016, 2007.

"Phase Transition Enthalpy Measurements of Organic and Organometallic Compounds" in NIST Chemistry WebBook, NIST Standard Reference Database Number 69, last

Zhao, J. and Zhang, R.: Proton transfer reaction rate constants between hydronium ion (H3O+) and volatile organic compounds, Atmospheric Environment, 38, 2177-2185, https://doi.org/10.1016/j.atmosenv.2004.01.019, 2004.